International Journal of
Molecular Sciences

MDPI

Article

Beta-Caryophyllene, a Plant-Derived CB2 Receptor Agonist, Protects SH-SY5Y Cells from Cadmium-Induced Toxicity

Federica Mannino [1], Giovanni Pallio [2], Chiara Imbesi [1], Alessandro Scarfone [1], Domenico Puzzolo [2], Antonio Micali [3], José Freni [2], Francesco Squadrito [1], Alessandra Bitto [1], Letteria Minutoli [1,*] and Natasha Irrera [1]

[1] Department of Clinical and Experimental Medicine, University of Messina, 98125 Messina, Italy; fmannino@unime.it (F.M.); chimbesi@unime.it (C.I.); alessandro.scarfone@unime.it (A.S.); fsquadrito@unime.it (F.S.); abitto@unime.it (A.B.); nirrera@unime.it (N.I.)
[2] Department of Biomedical and Dental Sciences and Morphological and Functional Imaging, University of Messina, 98125 Messina, Italy; gpallio@unime.it (G.P.); puzzolo@unime.it (D.P.); jose.freni@unime.it (J.F.)
[3] Department of Adult and Childhood Pathology "Gaetano Barresi", University of Messina, 98125 Messina, Italy; amicali@unime.it
* Correspondence: lminutoli@unime.it

Abstract: Cadmium (Cd) is a transition heavy metal that is able to accumulate in the central nervous system and may induce cell death through reactive oxygen species (ROS)-mediated mechanisms and inactivating the antioxidant processes, becoming an important risk factor for neurodegenerative diseases. The antioxidant effects of cannabinoid receptor modulation have been extensively described, and, in particular, β-Caryophyllene (BCP), a plant-derived cannabinoid 2 receptor (CB2R) agonist, not only showed significant antioxidant properties but also anti-inflammatory, analgesic, and neuroprotective effects. Therefore, the aim of the present study was to evaluate BCP effects in a model of Cd-induced toxicity in the neuroblastoma SH-SY5Y cell line used to reproduce Cd intoxication in humans. SH-SY5Y cells were pre-treated with BCP (25, 50, and 100 μM) for 24 h. The day after, cells were challenged with cadmium chloride ($CdCl_2$; 10 μM) for 24 h to induce neuronal toxicity. $CdCl_2$ increased ROS accumulation, and BCP treatment significantly reduced ROS production at concentrations of 50 and 100 μM. In addition, $CdCl_2$ significantly decreased the protein level of nuclear factor erythroid 2–related factor 2 (Nrf2) compared to unstimulated cells; the treatment with BCP at a concentration of 50 μM markedly increased Nrf2 expression, thus confirming the BCP anti-oxidant effect. Moreover, BCP treatment preserved cells from death, regulated the apoptosis pathway, and showed a significant anti-inflammatory effect, thus reducing the pro-inflammatory cytokines increased by the $CdCl_2$ challenge. The results indicated that BCP preserved neuronal damage induced by Cd and might represent a future candidate for protection in neurotoxic conditions.

Keywords: cadmium; neurotoxicity; ROS; inflammation; beta-caryophyllene

Citation: Mannino, F.; Pallio, G.; Imbesi, C.; Scarfone, A.; Puzzolo, D.; Micali, A.; Freni, J.; Squadrito, F.; Bitto, A.; Minutoli, L.; et al. Beta-Caryophyllene, a Plant-Derived CB2 Receptor Agonist, Protects SH-SY5Y Cells from Cadmium-Induced Toxicity. *Int. J. Mol. Sci.* **2023**, *24*, 15487. https://doi.org/10.3390/ijms242015487

Academic Editor: Stephen C. Bondy

Received: 3 October 2023
Revised: 17 October 2023
Accepted: 20 October 2023
Published: 23 October 2023

1. Introduction

Heavy metals are chemical elements characterized by high density compared to water and are responsible for toxicity in humans [1]; in fact, heavy metals exposure is an increasing worldwide concern for ecological and public health fields [2]. Some metals, such as iron (Fe), magnesium (Mg), manganese (Mn), selenium (Se), and zinc (Zn), are considered essential nutrients useful for biochemical and physiological functions so that their inadequate supplementation might be responsible for deficiency diseases or syndromes [3]; on the contrary, no biological function has been demonstrated for other metals that are considered non-essential metals, such as lead (Pb), mercury (Hg), and cadmium (Cd) [4].

Cd is a transition metal whose exposure depends on inhalation and ingestion, as well as cigarette smoke. Cd traces have been found in food (i.e., rice and grain), air pollution, and drinking water, which refer to non-occupational Cd exposure, but both non- and

occupational Cd exposure have been linked to toxicity phenomena in different tissues and to the appearance of different cancers [5,6]. Once absorbed, Cd is distributed by divalent metal transporter 1 (DMT1) and albumin, has a long half-life, and its renal excretion is very slow; for this reason, Cd traces may be detected in the body following 10–30 years from exposure [7,8]. In addition, Cd is able to cross the blood–brain barrier (BBB) and may accumulate in the central nervous system (CNS), thus inducing cell death in neurons and glial cells through reactive oxygen species (ROS)-mediated mechanisms [9,10]. The accumulation in the substantia nigra increases ROS production, becoming an important risk factor for neurodegenerative disease development, such as Parkinson's disease and Alzheimer's disease [11–13].

The mechanisms of Cd toxicity are not fully understood, even if different in vitro and in vivo studies indicated that they may induce inflammatory processes; in particular, ROS production is responsible for cell and single-strand DNA damage as well as disruption of nucleic acids and protein synthesis [14,15]. Furthermore, this heavy metal is able to inhibit mitochondrial enzymes, thus altering the mitochondrial membrane and inducing failure of cellular respiration with the consequent release of cytochrome C and caspases for apoptosis activation [16,17]. Different studies aimed at managing Cd toxicity, also by using compounds with antioxidant and anti-inflammatory effects [18,19], but until now the therapeutic options were mainly based on gastrointestinal tract irrigation and chemical decontamination and traditional-based chelation therapy with chelating agents and antidotes [20]. For this reason, the chance of finding alternative approaches still remains a challenge, and, in this context, cannabinoids (CBs) have recently proved to be effective in modulating oxidative stress and reducing inflammation [21]. Most of the effects of CBs and endocannabinoids are mainly mediated by two G protein-coupled receptors (GPCRs), CB1 and CB2, widely distributed in the body [22]. In this setting, β-Caryophyllene (BCP), a plant-derived cannabinoid 2 receptor (CB2R) agonist, showed significant anti-inflammatory, antioxidant, and analgesic properties in different experimental models, as well as neuroprotective effects [23,24]. Moreover, previous studies demonstrated that BCP was effective in reducing oxidative stress and toxicity induced by Cd, at least in the male reproductive system and in a *Caenorhabditis elegans* model system [25,26].

The aim of the present study was to evaluate the neuroprotective effects of BCP in a model of toxicity induced by Cd, as cadmium chloride ($CdCl_2$), in a human neuroblastoma SH-SY5Y cell line used to reproduce Cd intoxication in humans.

2. Results

2.1. BCP Treatment Does Not Influence SH-SY5Y Cell Viability

SH-SY5Y cell viability was evaluated following the treatment with doubling concentrations of BCP, starting from 6.25 μM up to 200 μM. The results of the MTT assay showed that BCP did not affect cell viability at all tested concentrations (Figure 1); therefore, the concentrations of 25, 50, and 100 μM were chosen in accordance with previous experiments [27].

2.2. BCP Protects SH-SY5Y Cells from the Damage Induced by $CdCl_2$

In undifferentiated SH-SY5Y cells, control cells were numerous and arranged in clusters; they showed the typical flat morphology with short, stubby processes. and euchromatic nuclei with evident nucleoli; occasional mitoses were also observed (Figure 2A,F). A sharp reduction in the number of cells/unit area (UA) was observed in $CdCl_2$-challenged cells (Figure 2B,F). Cells showed heterochromatic nuclei and reduced or absent processes; no mitoses were detected, and some nuclei showed apoptotic bodies. A significant increase in the number of cells/UA was evident in $CdCl_2$ samples treated with BCP at a concentration of 25 μM (Figure 2C,F); cells showed either heterochromatic or euchromatic nuclei with evident nucleoli. Furthermore, occasional necrotic cells and apoptotic bodies were also present. BCP at a concentration of 50 μM increased the number of cells/UA (Figure 2D,F), as demonstrated by the augmented number of cells with euchromatic nuclei compared

to those with heterochromatic nuclei. Moreover, both apoptotic and dividing cells were observed. A further increase in cells arranged in clusters was evident in $CdCl_2$-challenged cells treated with BCP at a concentration of 100 μM with a morphological pattern similar to controls (Figure 2E,F). Mitoses were present in many microscopic fields.

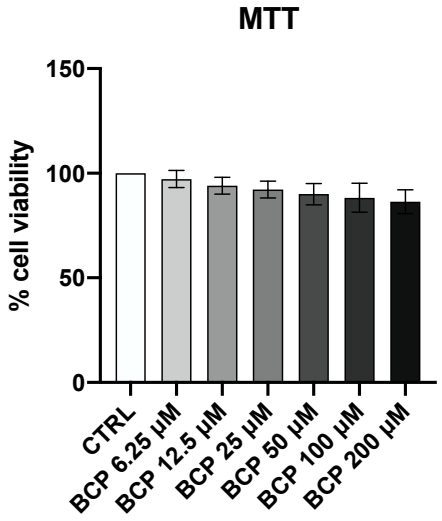

Figure 1. Cytotoxicity assay evaluated in SH-SY5Y cell line treated with BCP at concentrations of 6.25, 12.5, 25, 50, 100, and 200 μM for 24 h. Values are expressed as the means ± SD of three experiments.

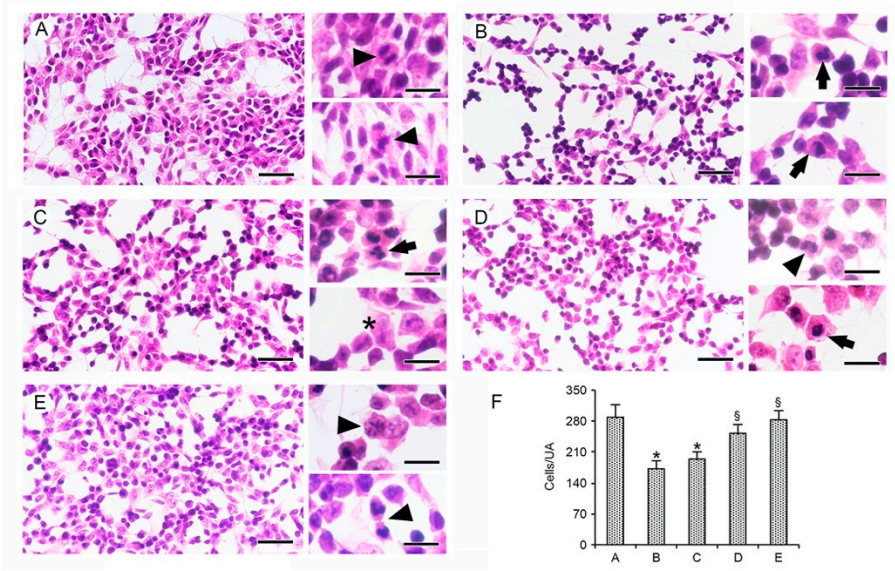

Figure 2. Representative morphological images of undifferentiated SH-SY5Y cells challenged with $CdCl_2$ and treated with different doses of β-caryophyllene (BCP). (**A**): Clusters of round control cells with euchromatic nuclei and short processes, particularly evident in the edges of the clusters. Occasional mitoses are present (arrowheads). (**B**): Cells challenged with $CdCl_2$ alone. Note the presence of heterochromatic or apoptotic (arrows) nuclei, the reduction in processes, and the absence of mitoses. (**C**): Cells challenged with $CdCl_2$ and treated with 25 μM of BCP. Euchromatic, heterochromatic, and apoptotic (arrow) nuclei, and occasional necrotic cells (*) are present. (**D**): Cells challenged with $CdCl_2$ and treated with 50 μM of BCP. Both mitotic (arrowhead) and apoptotic (arrow) cells are present. (**E**): Cells challenged with $CdCl_2$ and treated with 100 μM of BCP are arranged in clusters and show a morphological pattern similar to controls, with occasional mitoses (arrowheads). (Hematoxylin and Eosin stain. Scale bar = 50 μm; insets = 25 μm). (**F**): Mean number of undifferentiated SH-SY5Y cells/UA in the different groups examined. A = control; B = $CdCl_2$-challenged cells; C = $CdCl_2$-challenged cells treated with BCP 25 μM; D = $CdCl_2$-challenged cells treated with BCP 50 μM; E = $CdCl_2$-challenged cells

treated with BCP 100 μM. Data are expressed as mean ± SD. * $p \leq 0.05$ versus controls; § $p \leq 0.05$ versus $CdCl_2$-challenged cells.

In SH-SY5Y cells differentiated with retinoic acid (RA), no clusters were present (Figure 3A). Cells were less numerous/UA when compared to control undifferentiated cells (Figure 3F) and generally isolated. Elongated or pyramidal bodies were detected, with evident processes and euchromatic nuclei (Figure 3A); no mitoses were observed. RA-differentiated cells challenged with $CdCl_2$ showed a significant increase in their number/UA (Figure 3F), a round shape with heterochromatic nuclei, and a reduction in their processes; in particular, some nuclei exhibited apoptotic bodies (Figure 3B). In $CdCl_2$-challenged samples differentiated with RA and treated with BCP at a concentration of 25 μM, a mild and not significant increase in the number of cells (Figure 3F) with either euchromatic or heterochromatic nuclei was observed; occasional apoptotic bodies were also detected (Figure 3C). BCP at the concentration of 50 μM induced a significant reduction in the number/UA (Figure 3F) of RA-differentiated cells challenged with $CdCl_2$, which showed euchromatic nuclei and some short processes (Figure 3D); additionally, some apoptotic cells were also present. $CdCl_2$-challenged cells differentiated with RA and treated with BCP at a concentration of 100 μM showed both cell number/UA and morphological pattern similar to controls, with evident processes (Figure 3E,F).

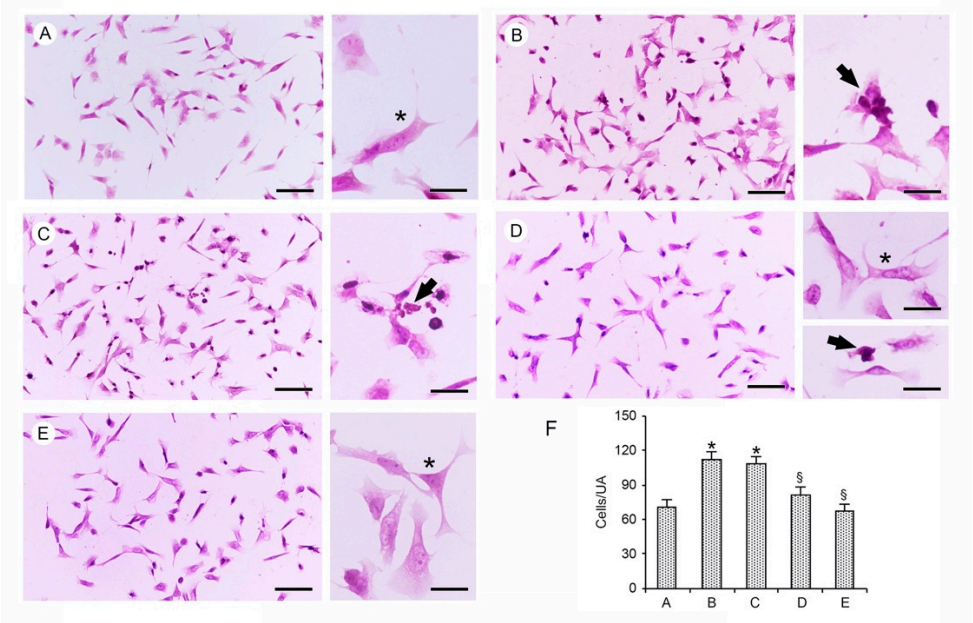

Figure 3. Representative morphological images of SH-SY5Y cells differentiated with RA, challenged with $CdCl_2$, and treated with different doses of BCP. (**A**): Cells differentiated with RA (controls) are isolated, with elongated or pyramidal bodies and evident processes (*). (**B**): RA-differentiated cells challenged with $CdCl_2$ show round shape, heterochromatic nuclei, and few processes. Some cells have apoptotic bodies (arrow). (**C**): In $CdCl_2$-challenged cells differentiated with RA and treated with BCP at 25 μM, either euchromatic or heterochromatic nuclei are present; occasional apoptotic bodies are evident (arrow). (**D**): $CdCl_2$-challenged cells differentiated with RA and treated with BCP at 50 μM show euchromatic nuclei and some short processes (*); some isolated apoptotic cells are present (arrow). (**E**): After treatment with BCP at the concentration of 100 μM, $CdCl_2$-challenged cells differentiated with RA show a morphological pattern similar to controls, with evident processes (*). (Hematoxylin and Eosin stain. Scale bar = 50 μm; insets = 25 μm). (**F**): Mean number of RA-differentiated SH-SY5Y cells/UA in the different groups examined. A = control; B = $CdCl_2$-challenged RA-differentiated cells; C = $CdCl_2$-challenged RA-differentiated cells treated with BCP 25 μM; D = $CdCl_2$-challenged RA-differentiated cells treated with BCP 50 μM; E = $CdCl_2$-challenged RA-differentiated cells treated with BCP 100 μM. Data are expressed as mean ± SD. * $p \leq 0.05$ versus controls; § $p \leq 0.05$ versus $CdCl_2$-challenged RA-differentiated cells.

2.3. BCP Reduces Intracellular ROS Production

Intracellular ROS production was evaluated to investigate the possible antioxidant effects of BCP, both in undifferentiated and differentiated SH-SY5Y cells. $CdCl_2$ induced a marked increase in fluorescence signal in both cell lines, thus indicating an increased ROS accumulation in $CdCl_2$-challenged cells compared to controls (Figures 4B and 5B). BCP significantly reduced ROS production at both concentrations of 50 and 100 µM (Figure 4D,E and Figure 5D,E), whereas a slight reduction in ROS levels was observed at the dose of 25 µM (Figures 4C and 5C).

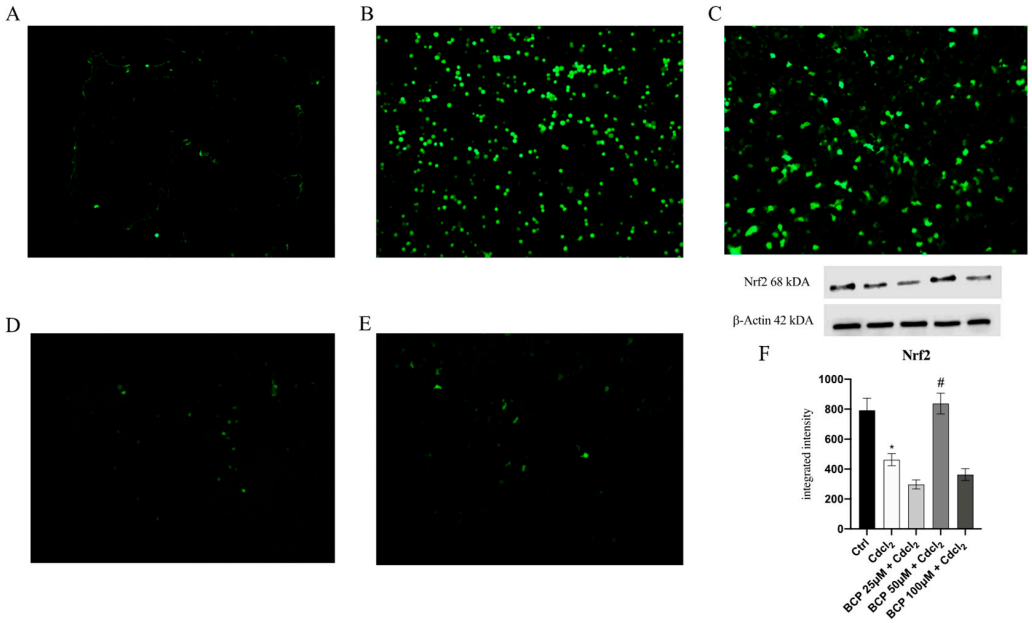

Figure 4. The panel shows intracellular ROS accumulation evaluated by CM-H2DCFDA probe in undifferentiated SH-SY5Y cell line from ctrl (**A**), $CdCl_2$ (**B**), $CdCl_2$ + BCP 25 µM (**C**), $CdCl_2$ + BCP 50 µM (**D**), and $CdCl_2$ + BCP 100 µM (**E**). The graph (**F**) shows Nrf2 protein expression. The data are expressed as the means and SD of three experiments. * $p < 0.05$ vs. ctrl; # $p < 0.05$ vs. $CdCl_2$.

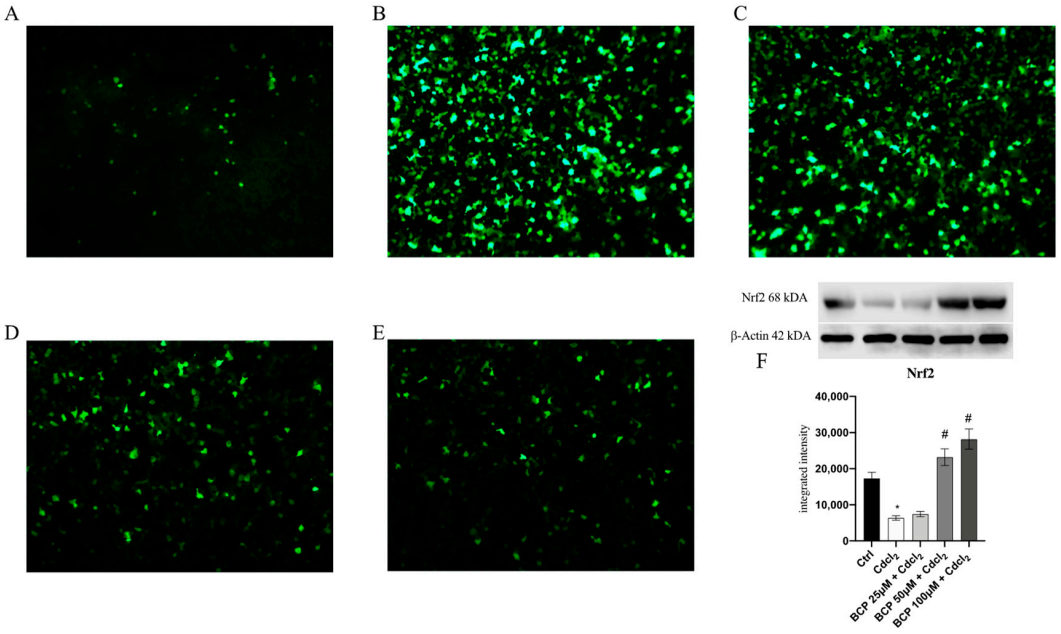

Figure 5. The panel shows intracellular ROS accumulation evaluated by CM-H2DCFDA probe in differentiated SH-SY5Y cell line from ctrl (**A**), $CdCl_2$ (**B**), $CdCl_2$ + BCP 25 µM (**C**), $CdCl_2$ + BCP 50 µM (**D**),

and $CdCl_2$ + BCP 100 µM (**E**). The graph (**F**) shows Nrf2 protein expression. The data are expressed as the means and SD of three experiments. * $p < 0.05$ vs. ctrl; # $p < 0.05$ vs. $CdCl_2$.

The BCP antioxidant effect was further confirmed by Western blot analysis by evaluating the nuclear factor erythroid 2–related factor 2 (Nrf2) expression. $CdCl_2$ significantly reduced the Nrf2 protein level in both undifferentiated and differentiated SH-SY5Y cells compared to unchallenged cells ($p < 0.05$ vs. ctrl; Figures 4F and 5F). Nrf2 expression was significantly increased with BCP at the concentration of 50 µM in undifferentiated SH-SY5Y cells ($p < 0.05$ vs. $CdCl_2$; Figure 4F), whereas a significant increase in its expression was observed at the concentrations of 50 and 100 µM in differentiated SH-SY5Y cells ($p < 0.05$ vs. $CdCl_2$; Figure 5F), thus confirming the BCP anti-oxidant effect.

2.4. BCP Treatment Inhibits Cell Death and Reduces Pro-Inflammatory Cytokines Expression following $CdCl_2$ Stimulation

Both Bcl-2-associated X protein (Bax) and B-cell lymphoma 2 (Bcl-2) protein expression were investigated by Western blot analysis to evaluate whether BCP was able to modulate apoptosis. $CdCl_2$ induced the pro-apototic Bax expression and reduced Bcl-2 expression, a well-established anti-apoptotic marker, compared to untreated cells in both cell lines ($p < 0.05$ vs. ctrl; Figure 6). The data obtained following BCP treatment showed that this CB2 agonist protects cells from Cd-induced apoptosis, thus reducing Bax and increasing Bcl-2 expression, mostly when BCP was used at a concentration of 100 µM ($p < 0.05$ vs. $CdCl_2$; Figure 6).

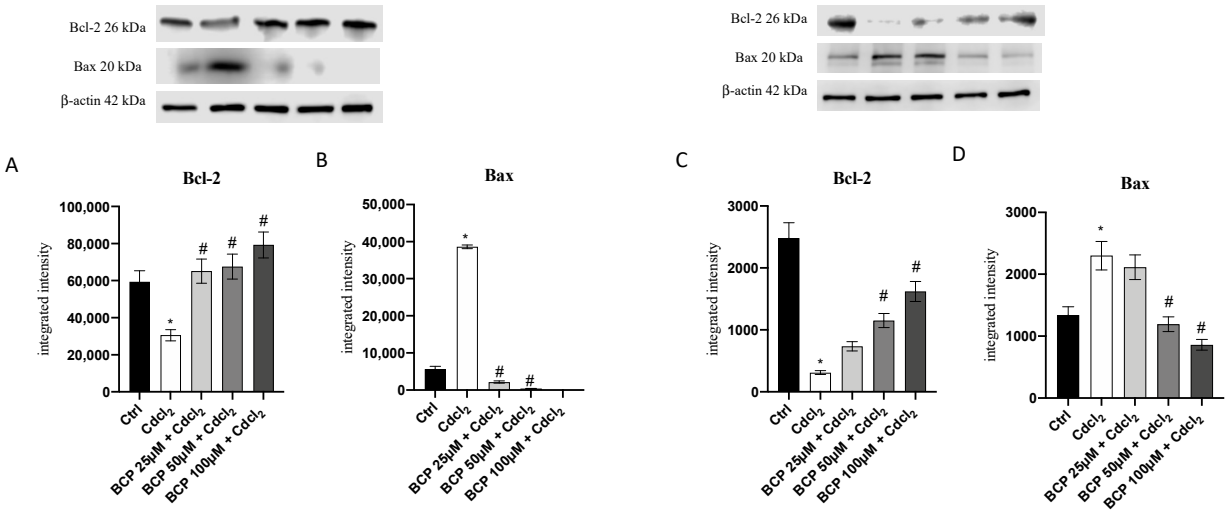

Figure 6. The graphs represent Bcl-2 (**A**) and Bax (**B**) protein expression in undifferentiated SH-SY5Y cells and Bcl-2 (**C**) and Bax (**D**) in differentiated SH-SY5Y cells. The data are expressed as the means and SD of three experiments. * $p < 0.05$ vs. ctrl; # $p < 0.05$ vs. $CdCl_2$.

The anti-apoptotic effects of BCP were also evaluated by the terminal deoxynucleotidyl transferase dUTP nick end labeling (TUNEL) assay; no positive cells were observed in undifferentiated SH-SY5Y cells (Figure 7A,F). A significant increase in positive cell number was observed in cells challenged with $CdCl_2$ (Figure 7B,F). BCP at a concentration of 25 µM significantly reduced the number of positive cells (Figure 7C,F), and a further reduction was observed following BCP treatment at a concentration of 50 µM (Figure 7D,F). Only isolated positive cells were observed when BCP was used at a concentration of 100 µM (Figure 7E,F).

All controls were negative in RA-differentiated SH-SY5Y cells (Figure 8A,F), whereas $CdCl_2$ induced a dramatic increase in positive cells (Figure 8B,F), which was significantly reduced after treatment with BCP at 25 µM (Figure 8C,F) and 50 µM (Figure 8D,F). Only following the use of BCP 100 µM, isolated positive cells were observed (Figure 8E,F).

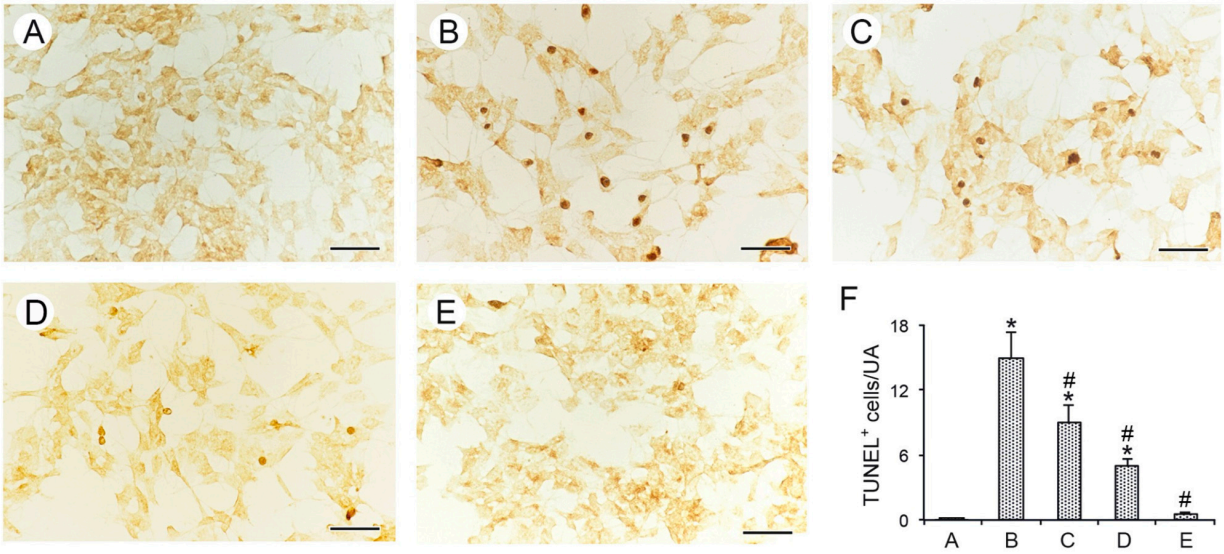

Figure 7. Assessment of apoptosis with TUNEL staining technique in undifferentiated SH-SY5Y cells challenged with $CdCl_2$ after treatment with different doses of BCP. (**A**): No TUNEL-positive cells are present in control cells. (**B**): Cells challenged with $CdCl_2$ alone. A large number of TUNEL-positive cells are present. (**C**): Cells challenged with $CdCl_2$ and treated with 25 μM of BCP. Many TUNEL-positive cells are observed. (**D**): Cells challenged with $CdCl_2$ and treated with 50 μM of BCP. An evident reduction in TUNEL-positive cells is present. (**E**): Cells challenged with $CdCl_2$ and treated with 100 μM of BCP. Only isolated TUNEL-positive cells are present. (**F**): Mean number of cells/UA in the different groups examined. Data are expressed as mean ± SD of three experiments. * $p \leq 0.05$ vs. ctrl; # $p < 0.05$ vs. $CdCl_2$. Scale bar = 50 μm.

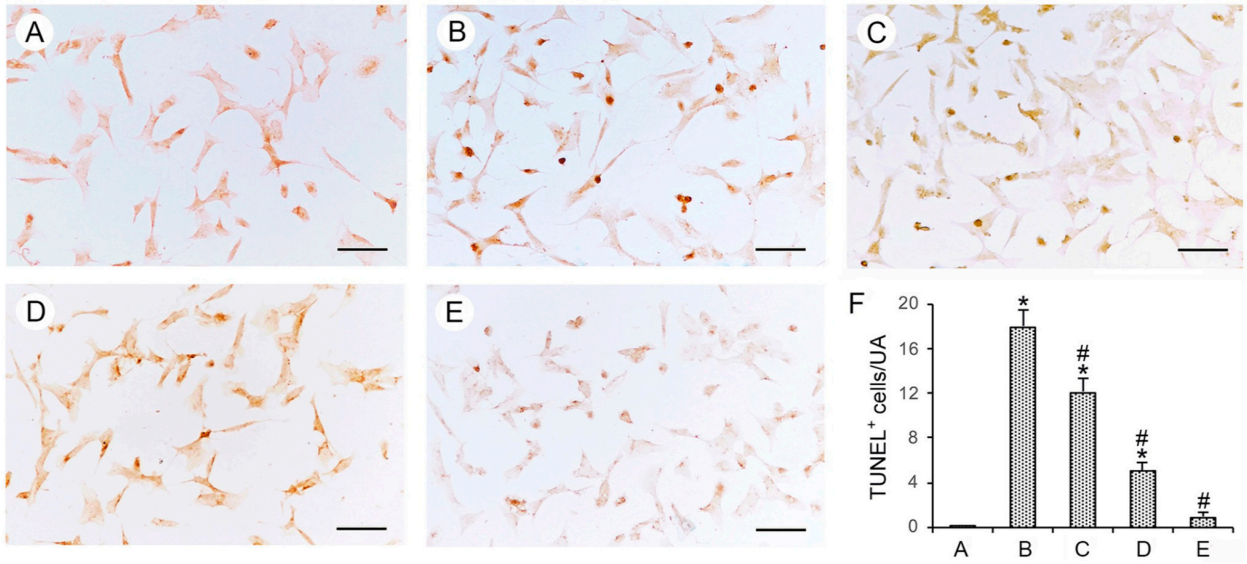

Figure 8. Assessment of apoptosis with TUNEL staining technique in RA-differentiated SH-SY5Y cells challenged with $CdCl_2$ and treated with different doses of BCP. (**A**): No positive cells are present in RA-differentiated control cells. (**B**): RA-differentiated cells challenged with $CdCl_2$ alone show a large number of positive cells. (**C**): In RA-differentiated cells challenged with $CdCl_2$ and treated with 25 μM of BCP many positive cells are observed. (**D**): RA-differentiated cells challenged with $CdCl_2$ and treated with 50 μM of BCP show an evident reduction in positive cells. (**E**): Only isolated positive cells are present in RA-differentiated cells challenged with $CdCl_2$ and treated with 100 μM of BCP. (**F**): Mean number of TUNEL-positive cells/UA in the different groups of RA-differentiated cells examined. Data are expressed as mean ± SD. * $p \leq 0.05$ versus controls; # $p \leq 0.05$ versus $CdCl_2$-challenged cells. Scale bar = 50 μm.

In addition, *interleukin (IL)-6*, *IL-1β*, and *Tumor Necrosis Factor (TNF)-α* gene expression was evaluated by qPCR to confirm the well-known BCP anti-inflammatory effect (Figures 9 and 10). $CdCl_2$ challenge induced inflammation in both undifferentiated and differentiated SH-SY5Y cells, as demonstrated by the increased expression of the pro-inflammatory cytokines. BCP treatment significantly reduced *IL-6*, *IL-1β*, and *TNF-α* gene expression at all tested concentrations, but mostly following the treatment with BCP 100 μM (* $p < 0.05$ vs. ctrl; # $p < 0.05$ vs. $CdCl_2$), thus demonstrating BCP anti-inflammatory effects also in this experimental setting.

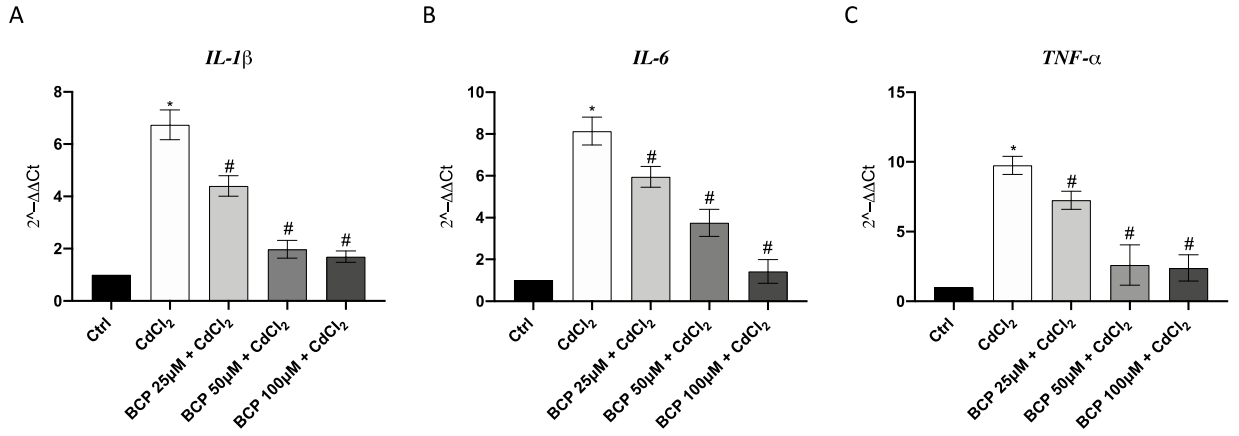

Figure 9. The graphs represent *IL-1β* (**A**), *IL-6* (**B**), and *TNF-α* (**C**) mRNA expression assessed by RT-PCR in undifferentiated SH-SY5Y cells. The data are expressed as the means and SD of three experiments. * $p < 0.05$ vs. CTRL; # $p < 0.05$ vs. $CdCl_2$.

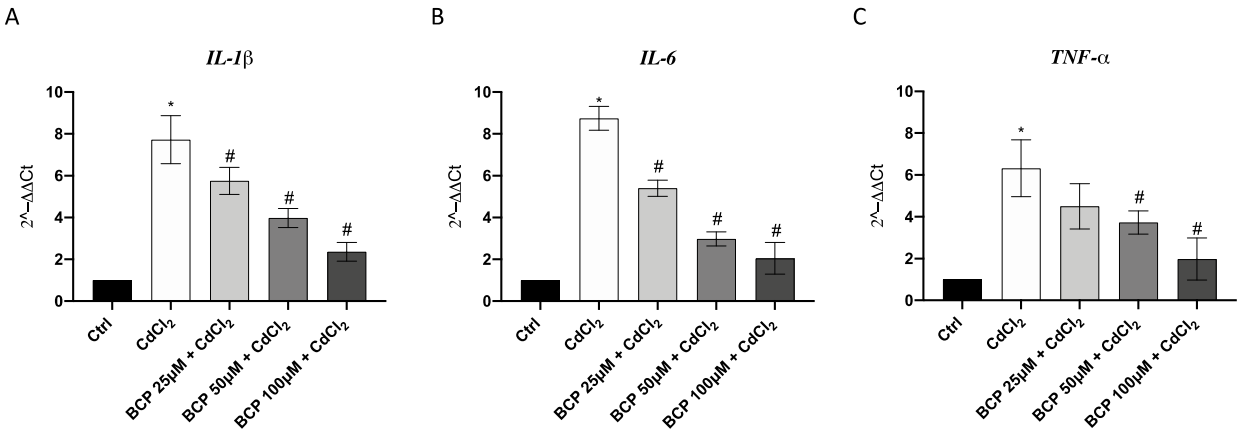

Figure 10. The graphs represent *IL-1β* (**A**), *IL-6* (**B**), and *TNF-α* (**C**) mRNA expression assessed by RT-PCR in differentiated SH-SY5Y cells. The data are expressed as the means and SD of three experiments. * $p < 0.05$ vs. ctrl; # $p < 0.05$ vs. $CdCl_2$.

3. Discussion

Cd is a widespread toxic pollutant with a long biological half-life in humans (20–30 years) and low-rate excretion that may induce neurodegeneration and memory impairment; in fact, its accumulation contributes to aging, as well as the onset of neurodegenerative diseases. Cd acts in the brain as a neurotoxin thanks to its ability to cross the BBB, thus inducing neurotoxicity phenomena [28,29] related to oxidative stress, neuroinflammation, and cell death mechanism activation [30,31]. Cd is able to modify the mitochondrial electron transport chain, thus triggering ROS release and oxidative stress stimulation [32], with the consequent activation of antioxidant molecules as scavengers of free radicals. In this experimental setting, $CdCl_2$ was used at a concentration of 10 μM to reproduce an in vitro model of Cd-induced

toxicity in SH-SY5Y cells that could mimic an in vivo chronic exposure in the brain. We demonstrated that the $CdCl_2$ challenge significantly induced oxidative stress, thus increasing ROS release compared to controls. The antioxidant effects of CB receptor modulation were extensively described; in particular, previous studies showed that the agonist cannabidiol carried out its antioxidant effect by modulating Nrf2, which is involved in the transcription of genes encoding for antioxidant proteins [21]. CB1 and CB2 receptors are widely distributed, and given that SH-SY5Y cells express CB2R, the choice of BCP was based on its high selectivity toward CB2R. Previous studies showed anti-oxidant, anti-inflammatory, and neuroprotective effects of BCP in other experimental models thanks to the modulation of different molecular pathways, such as those referred to CB2R and Peroxisome proliferator-activated receptor γ (PPARγ) activation [33,34]. First of all, we demonstrated that BCP use was safe as it did not induce mortality in SH-SY5Y cells; the concentrations of 25, 50, and 100 μM were selected to evaluate BCP neuroprotective effects [27]. BCP was not only able to reduce the release of ROS induced by $CdCl_2$ but also increased the impaired Nrf-2 expression in both undifferentiated and differentiated cell lines, thus confirming that BCP may act as an ROS scavenger and as a regulator of anti-oxidant systems. The mitochondrial ROS production induced by Cd may promote endoplasmic reticulum (ER) stress because of the physiological connection between mitochondria and ER, thus activating the pro-apoptotic protein Bax, which is a molecular signal of ER-stress-induced apoptosis [35,36]. In fact, $CdCl_2$ significantly reduced Bcl-2 expression and increased Bax in both cell lines, thus indicating that Cd induced apoptotic processes, as also confirmed by a TUNEL assay that revealed a significant increase in TUNEL-positive cells after $CdCl_2$ challenge compared to control cells. Cell death mechanisms, including autophagy and apoptosis, may be regulated by different signal transduction pathways, including those deriving from CB1 and CB2 receptors, which are expressed in neuronal cells [37–39]. In this context, BCP, an agonist of CB2R, preserved undifferentiated SH-SY5Y cells and SH-SY5Y cells differentiated with RA from apoptosis by modulating Bax and Bcl-2 expression, and in particular, BCP significantly reduced Bax expression at a concentration of 100 μM. BCP anti-apoptotic effects were also microscopically observed through the reduction in TUNEL-positive cells compared to untreated cells stimulated with $CdCl_2$. Cd-induced neuronal apoptosis might be reversed by inhibiting ROS production and neuroinflammation, as previously demonstrated in several papers that investigated the effects of natural antioxidant compounds against Cd-induced neurotoxicity [40,41]. The increased ROS production may also promote the nuclear factor-kappa B (NF-κB) translocation from cytoplasm to nucleus that represents a trigger for the activation of mRNA expression transcription of different pro-inflammatory cytokines [42]. In accordance with other studies [43,44], we demonstrated that $CdCl_2$ caused neuroinflammation, as observed by the increased levels of *TNF-α*, *IL-1β*, and *IL-6* in both cell lines. BCP not only showed anti-oxidant effects through scavenging impaired ROS production but also significantly reduced pro-inflammatory markers, thus confirming its already known anti-inflammatory effects. In summary, the results described so far demonstrated that BCP was protective against $CdCl_2$-induced damage in undifferentiated SH-SY5Y cells and SH-SY5Y cells differentiated with RA. This neuroprotective effect is the result of oxidative stress, neuroinflammation, and apoptosis inhibition. Although these results would need further in vitro and in vivo investigations, BCP could be proposed as a future candidate for neuroprotection.

4. Materials and Methods

4.1. Cell Culture

Human neuroblastoma SH-SY5Y cell line was purchased by ATCC (CRL-2266™; Manassas, VA, USA). Cells were cultured in DMEM (Dulbecco's Modified Eagle Medium) High Glucose/Ham's F12 Mixture Medium (1:1 ratio), supplemented with 10% fetal bovine serum (FBS), 2 mM L-Glutamine, 1% antibiotic mixture (Sigma-Aldrich, St. Louis, MO, USA), in a humidified incubator at 37 °C and with 5% CO_2.

4.2. Cell Treatment

SH-SY5Y neuroblast-like cells were plated in a 6-well plate at a density of 1×10^5 cells/well and incubated at 37 °C with a percentage of 5% CO_2 overnight. The day after, cells were differentiated in neuron-like cells. In particular, 10 μM of retinoic acid (RA) was added to each well for five days and the medium was changed every two days. At day 6, RA was removed, cells were washed three times with sterile phosphate-buffered saline (PBS) and brain-derived neurotrofic factor (BDNF; 50 ng/mL) was added for additional five days in order to improve RA effects on neuronal differentiation.

Undifferentiated SH-SY5Y cells and neuron cells were cultured in 6-well plates at a density of 2.5×10^5 cells/well; 24 h after seeding, cells were pre-treated with β-caryophyllene (BCP) (Sigma-Aldrich, St. Louis, MO, USA) at the concentrations of 25, 50 and 100 μM for 24 h. The day after, the medium was replaced and the cells were stimulated with 10 μM of cadmium chloride ($CdCl_2$) (Sigma-Aldrich, St. Louis, MO, USA) for additional 24 h in order to reproduce an in vitro model of Cd-induced neuronal toxicity, as previously reported [45]. All treatments were performed in starvation conditions because essential elements of medium, such as zinc and calcium, could compromise Cd effects. At the end of the incubation period, cells were collected for molecular and morphological analyses.

4.3. MTT Assay

MTT assay was performed to evaluate BCP effects on cell viability. SH-SY5Y were seeded in a 96-well plate at a density of 1×10^5 cells/well for 24 h. The day after, cells were treated with doubling concentrations of BCP (6.25, 12.5, 25, 50, 100, and 200 μM) for 24 h. Five hours before the end of the treatment, 20 μL of 3-(4,5-dimethylthiazol-2yl)-2,5-diphenyl tetrazolium bromide (MTT) solution (Sigma-Aldrich, St. Louis, MO, USA) (0.5 mg/mL) was added into each well. 200 μL of dimethyl sulfoxide (DMSO; Sigma-Aldrich, St. Louis, MO, USA) were added into each well to dissolve the insoluble formazan crystals. The reaction was read at 540 and 620 nm of absorbance by using VICTOR Multilabel Plate Reader (Perkin Elmer; Waltham, MA, USA), and the results were expressed as % of cell viability compared to untreated cells and reported as means and standard deviation (SD) [46].

4.4. Hematoxylin/Eosin Staining

The cells from both undifferentiated and RA-differentiated cells were fixed in 4% paraformaldehyde, washed in PBS, stained with hematoxylin and eosin (HE), and photographed with a Nikon Ci-L light microscope (Nikon Instruments, Tokyo, Japan). The images were obtained with a digital camera (Nikon DS-Ri2).

4.5. Evaluation of Apoptosis with Terminal Deoxynucleotidyl Transferase dUTP Nick End Labeling (TUNEL) Assay

An apoptosis detection kit (in situ Apoptosis Detection kit, Abcam, Cambridge, UK) was used for the TUNEL technique following the manufacturer's instructions. In brief, cells from both undifferentiated and RA-differentiated cells were fixed in 4% paraformaldehyde, washed in PBS, and endogenous peroxidase activity was blocked with 3% H_2O_2 in methanol after permeabilization with proteinase K. Samples were incubated with terminal deoxynucleotidyl transferase, biotin-labeled deoxynucleotides, streptavidin-horseradish peroxidase conjugate, and lastly with the diaminobenzidine solution. No counterstaining was performed to better observe apoptotic cells. Cells were photographed with a Nikon Ci-L light microscope using a digital camera, the Nikon Ds-Ri2 [47].

4.6. Morphometric Evaluation

All images were saved as Tagged Image Format Files (TIFF), printed at the same final magnification, and blindly assessed by two trained observers. As to the specimens from both undifferentiated and RA-differentiated cells stained with HE, the mean number of cells per Unit Area (UA = 250 × 250 μm) was calculated from 20 UAs for each experimental group, obtained from micrographs taken with an objective of 20×. In order to evaluate

apoptosis in both undifferentiated and RA-differentiated cells, the mean number of TUNEL-positive cells/UA was calculated from 20 UAs (UA = 250 × 250 μm) for each group, obtained from micrographs taken with an objective of 20×. In both procedures, cells overlapping the right and top boundaries were not included in the evaluation, whereas cells overlapping the left and bottom boundaries were counted.

4.7. Measurement of ROS Production

ROS production was studied by using the probe 5-(and-6)-chloromethyl-2′, 7′-dichlorodihydrofluorescein diacetate (CM-H2DCFDA) (Thermofisher, Waltham, MA, USA). At the end of the treatment period, SH-SY5Y cells and neuron-like cells were incubated with 5 μM of CM-H2DCFDA for 1 h at 37 °C. Cells were then washed with PBS to remove the excess probe and observed with a fluorescent microscope at 10× magnification. The signal of fluorescence was quantified with ImageJ software for Windows (Softonic, Barcelona, Spain) [48].

4.8. RNA Isolation, cDNA Synthesis, and Real-Time Quantitative PCR Amplification

Total RNA was extracted from both cell lines using Trizol LS Reagent Kit (Life Technologies, Monza, Italy) and quantified with a spectrophotometer (NanoDrop Lite, Thermo Fisher, Waltham, CA, USA). 1.0 μg of total RNA was reverse transcribed in cDNA using the SuperScript IV Master Mix (Thermo Fisher, Carlsbad, CA, USA) and used for qPCR analysis to evaluate *IL-6*, *IL-1β*, and *TNF-α* gene expression using the BrightGreen 2X qPCR MasterMix-Rox (Applied Biological Materials, Vancouver, Canada) and the QuantStudio 6 Flex Real-Time PCR System (Applied Biosystems, CA, USA). *β-Actin* was used as a housekeeping gene, and the amplified PCR products were quantified by measuring the calculated cycle thresholds (CT) of target genes and *β-actin* mRNA. After normalization, the mean value of the normal control target levels was chosen as calibrator, and the results were expressed according to the $2^{-\Delta\Delta Ct}$ method as a fold change relative to normal controls. Primers used for targets and reference genes are listed in Table 1 [49].

Table 1. Primer list.

Gene	Sequence
β-Actin	Fw: 5′AGAGCTACGAGCTGCCTGAC3′
	Rw: 5′AGCACTGTGTTGGCGTACAG3′
IL-1β	Fw: 5′TGAGCTCGCCAGTGAAATGA3′
	Rw: 5′AGATTCGTAGCTGGATGCCG3′
TNF-α	Fw: 5′CAGAGGGCCTGTACCTCATC3′
	Rw: 5′GGAAGACCCCTCCCAGATAG3′
IL-6	Fw: 5′TTCGGTCCAGTTGCCTTCTC3′
	Rw: 5′CAGCTCTGGCTTGTTCCTCA3′

4.9. Western Blot Analysis

At the end of the experimental procedure, SH-SY5Y cells and neuron-like cells were collected and homogenized in RIPA buffer (25 mM Tris/HCl, pH 7.4; 1.0 mM EGTA (Ethylene glycol bis(2-aminoethyl ether)-N,N,N′,N′-tetraacetic acid); 1.0 mM EDTA(Ethylenediaminetetraacetic acid dipotassium salt dihydrate) with NP40 (1%), phenyl methylsulfonyl fluoride (PMSF, 0.5%), aprotinin, leupeptin, and pepstatin (10 μM each)) and centrifuged at 15,000× *g* for 15 min at 4 °C; the supernatant obtained from each sample was used to measure the total protein content using the Bio-Rad protein-assay kit (BioRad, Hercules, CA, USA). 30 μg of proteins were run in a 10% sodium dodecyl sulphate (SDS) polyacrylamide gel and then transferred to PVDF membranes using a specific transfer buffer (39 mmol/L glycine, 48 mmol/L Tris, pH 8.3, and 20% methanol) at 300 mA for 2 h. The obtained membranes were blocked with 5% non-fat dry

milk in Tris buffered saline (TBS) 0.1% for 1 h at room temperature and incubated with primary antibodies for Bax and Nrf2 (Cell Signaling, Danvers, MA, USA) and Bcl-2 (Abcam, Cambridge, UK) diluted in TBS-0.1% Tween, overnight, at 4 °C. The day after, membranes were washed with TBS-0.1% Tween and incubated with a secondary peroxidase-conjugated goat anti-rabbit antibody (KPL, Gaithersburg, MD, USA) for 1 h at room temperature. After washing with TBS-0.15% Tween buffer, membranes were analyzed by the enhanced chemiluminescence system (LumiGlo reserve; Seracare, Milford, MA, USA). The protein signal was detected and quantified by scanning densitometry using a bio-image analysis system (C-DiGit, Li-cor, Lincoln, NE, USA). Results were expressed as relative integrated intensity, and β-actin (Cell Signaling, Danvers, MA, USA) was used to confirm equal protein loading in all samples [27].

4.10. Statistical Analysis

All the results are expressed as mean ± standard deviation (SD). The reported values are the results of at least three experiments. All assays were performed in duplicate to ensure reproducibility. Different groups were analyzed by One-Way ANOVA with Tukey's post-test for intergroup comparisons. A p value ≤ 0.05 was considered significant. Statistical analyses were performed using SPSS Statistics for MacOS v27.0 (SPSS, Inc., Chicago, IL, USA), and graphs were drawn with GraphPad Prism (Version 8.0 for MacOS, San Diego, CA, USA).

Author Contributions: Conceptualization, N.I.; supervision N.I. and L.M.; writing—original draft, F.M.; writing—review and editing, N.I. and F.S.; methodology, A.M., D.P. and A.B.; validation, C.I., A.S., J.F. and G.P. All authors have read and agreed to the published version of the manuscript.

Funding: This research received no external funding.

Institutional Review Board Statement: Not applicable.

Informed Consent Statement: Not applicable.

Data Availability Statement: The data presented in this study are available on request from the corresponding author.

Conflicts of Interest: The authors declare no conflict of interest.

References

1. Jaishankar, M.; Tseten, T.; Anbalagan, N.; Mathew, B.B.; Beeregowda, K.N. Toxicity, mechanism and health effects of some heavy metals. *Interdiscip. Toxicol.* **2014**, *7*, 60–72. [CrossRef]
2. Tchounwou, P.B.; Yedjou, C.G.; Patlolla, A.K.; Sutton, D.J. Heavy metal toxicity and the environment. *Exp. Suppl.* **2012**, *101*, 133–164. [PubMed]
3. World Health Organization; International Atomic Energy Agency & Food; Agriculture Organization of the United Nations. Trace Elements in Human Nutrition and Health. *World Health Organization.* 1996. Available online: https://apps.who.int/iris/handle/10665/37931 (accessed on 17 October 2023).
4. Chang, L.W.; Magos, L.; Suzuki, T. (Eds.) *Toxicology of Metals*; CRC Press: Boca Raton, FL, USA, 1996.
5. Jiale, C.; Chao, Z.; Jinzhao, R.; Chunhua, Z.; Ying, G. Cadmium Bioavailability and Accumulation in Rice Grain are Controlled by pH and Ca in Paddy Soils with High Geological Background of Transportation and Deposition. *Bull. Environ. Contam. Toxicol.* **2021**, *106*, 92–98. [CrossRef] [PubMed]
6. Genchi, G.; Sinicropi, M.S.; Lauria, G.; Carocci, A.; Catalano, A. The Effects of Cadmium Toxicity. *Int. J. Environ. Res. Public Health* **2020**, *17*, 3782. [CrossRef]
7. Tallkvist, J.; Bowlus, C.L.; Lonnerdal, B. DMT1 gene expression and cadmium absorption in human absorptive enterocytes. *Toxicol. Lett.* **2001**, *122*, 171–177. [CrossRef] [PubMed]
8. Amzal, B.; Julin, B.; Vahter, M.; Wolk, A.; Johanson, G.; Akesson, A. Population toxicokinetic modeling of cadmium for health risk assessment. *Environ. Health Perspect.* **2009**, *117*, 1293–1301. [CrossRef] [PubMed]
9. Chen, X.; Wu, W.; Gong, B.; Hou, L.; Dong, X.; Xu, C.; Zhao, R.; Yu, Q.; Zhou, Z.; Huang, S.; et al. Metformin attenuates cadmium-induced neuronal apoptosis in vitro via blocking ROS-dependent PP5/AMPK-JNK signaling pathway. *Neuropharmacology* **2020**, *175*, 108065. [CrossRef]
10. Chen, L.; Xu, B.; Liu, L.; Luo, Y.; Zhou, H.; Chen, W.; Shen, T.; Han, X.; Kontos, C.D.; Huang, S. Cadmium induction of reactive oxygen species activates the mTOR pathway, leading to neuronal cell death. *Free Radic. Biol. Med.* **2011**, *50*, 624–632. [CrossRef]
11. Chin-Chan, M.; Navarro-Yepes, J.; Quintanilla-Vega, B. Environmental pollutants as risk factors for neurodegenerative disorders: Alzheimer and Parkinson diseases. *Front. Cell. Neurosci.* **2015**, *9*, 124. [CrossRef]

12. Tönnies, E.; Trushina, E. Oxidative Stress, Synaptic Dysfunction, and Alzheimer's Disease. *J. Alzheimers Dis.* **2017**, *57*, 1105–1121. [CrossRef]
13. Li, X.; Lv, Y.; Yu, S.; Zhao, H.; Yao, L. The effect of cadmium on Abeta levels in APP/PS1 transgenic mice. *Exp. Ther. Med.* **2012**, *4*, 125–130. [CrossRef] [PubMed]
14. Stohs, S.J.; Bagchi, D. Oxidative mechanisms in the toxicity of metal ions. *Free Radic. Biol. Med.* **1995**, *18*, 321–336. [CrossRef] [PubMed]
15. Mitra, R.S. Protein synthesis in Escherichia coli during recovery from exposure to low levels of Cd2+. *Appl. Environ. Microbiol.* **1984**, *47*, 1012–1016. [CrossRef] [PubMed]
16. Belyaeva, E.A.; Dymkowska, D.; Wieckowski, M.R.; Wotczak, L. Reactive oxygen species produced by the mitochondrial respiratory chain are involved in Cd2+-induced injury of rat ascites hepatoma AS-30D cells. *Biochim. Biophys. Acta* **2006**, *1757*, 1568–1574. [CrossRef] [PubMed]
17. Chatterjee, S.; Kundu, S.; Bhattacharyya, A. Mechanism of cadmium induced apoptosis in the immunocyte. *Toxicol. Lett.* **2008**, *177*, 83–89. [CrossRef] [PubMed]
18. Nemmiche, S.; Chabane-Sari, D.; Guiraud, P. Role of alpha-tocopherol in cadmium-induced oxidative stress in Wistar rat's blood, liver and brain. *Chem. Biol. Interact.* **2007**, *170*, 221–230. [CrossRef]
19. Abdel Moneim, A.E.; Bauomy, A.A.; Diab, M.M.; Shata, M.T.; Al-Olayan, E.M.; El-Khadragy, M.F. The protective effect of Physalis peruviana L. against cadmium-induced neurotoxicity in rats. *Biol. Trace Elem. Res.* **2014**, *160*, 392–399. [CrossRef]
20. Rafati Rahimzadeh, M.; Rafati Rahimzadeh, M.; Kazemi, S.; Moghadamnia, A.A. Cadmium toxicity and treatment: An update. *Casp. J. Intern. Med.* **2017**, *8*, 135–145.
21. Atalay, S.; Jarocka-Karpowicz, I.; Skrzydlewska, E. Antioxidative and Anti-Inflammatory Properties of Cannabidiol. *Antioxidants* **2019**, *9*, 21. [CrossRef]
22. Lutz, B. Neurobiology of cannabinoid receptor signaling. *Dialogues Clin. Neurosci.* **2020**, *22*, 207–222. [CrossRef]
23. Irrera, N.; D'Ascola, A.; Pallio, G.; Bitto, A.; Mazzon, E.; Mannino, F.; Squadrito, V.; Arcoraci, V.; Minutoli, L.; Campo, G.M.; et al. β-Caryophyllene Mitigates Collagen Antibody Induced Arthritis (CAIA) in Mice Through a Cross-Talk between CB2 and PPAR-γ Receptors. *Biomolecules* **2019**, *9*, 326. [CrossRef] [PubMed]
24. Machado, K.D.C.; Islam, M.T.; Ali, E.S.; Rouf, R.; Uddin, S.J.; Dev, S.; Shilpi, J.A.; Shill, M.C.; Reza, H.M.; Das, A.K.; et al. A systematic review on the neuroprotective perspectives of beta-caryophyllene. *Phytother. Res.* **2018**, *32*, 2376–2388. [CrossRef] [PubMed]
25. Espinosa-Ahedo, B.A.; Madrigal-Bujaidar, E.; Sánchez-Gutiérrez, M.; Izquierdo-Vega, J.A.; Morales-González, J.A.; Madrigal-Santillán, E.O.; Álvarez-González, I. Potential protective effect of beta-caryophyllene against cadmium chloride-induced damage to the male reproductive system in mouse. *Reprod. Toxicol.* **2022**, *110*, 19–30. [CrossRef] [PubMed]
26. Srivastava, S.; Pant, A.; Trivedi, S.; Pandey, R. Curcumin and β-caryophellene attenuate cadmium quantum dots induced oxidative stress and lethality in *Caenorhabditis elegans* model system. *Environ. Toxicol. Pharmacol.* **2016**, *42*, 55–62. [CrossRef]
27. Mannino, F.; Pallio, G.; Corsaro, R.; Minutoli, L.; Altavilla, D.; Vermiglio, G.; Allegra, A.; Eid, A.H.; Bitto, A.; Squadrito, F.; et al. Beta-Caryophyllene Exhibits Anti-Proliferative Effects through Apoptosis Induction and Cell Cycle Modulation in Multiple Myeloma Cells. *Cancers* **2021**, *13*, 5741. [CrossRef] [PubMed]
28. Min, J.; Min, K.B. Blood Cadmium chloride levels and Alzheimer's disease mortality risk in older US adults. *Environ. Health* **2016**, *15*, 69. [CrossRef]
29. Wang, B.; Du, Y. Cadmium chloride and its neurotoxic effects. *Oxidative Med. Cell. Longev.* **2013**, *2013*, 898034. [CrossRef]
30. Yuan, Y.; Zhang, Y.; Zhao, S.; Chen, J.; Yang, J.; Wang, T.; Zou, H.; Wang, Y.; Gu, J.; Liu, X.; et al. Cadmium-induced apoptosis in neuronal cells is mediated by Fas/FasL-mediated mitochondrial apoptotic signaling pathway. *Sci. Rep.* **2018**, *8*, 8837. [CrossRef]
31. Huang, Y.; Dai, Y.; Li, M.; Guo, L.; Cao, C.; Huang, Y.; Ma, R.; Qiu, S.; Su, X.; Zhong, K.; et al. Exposure to cadmium induces neuroinflammation and impairs ciliogenesis in hESC-derived 3D cerebral organoids. *Sci. Total Environ.* **2021**, *797*, 149043. [CrossRef]
32. Branca, J.J.V.; Fiorillo, C.; Carrino, D.; Paternostro, F.; Taddei, N.; Gulisano, M.; Pacini, A.; Becatti, M. Cadmium-Induced oxidative stress: Focus on the central nervous system. *Antioxidants* **2020**, *9*, 492. [CrossRef]
33. Javed, H.; Azimullah, S.; Haque, M.E.; Ojha, S.K. Cannabinoid Type 2 (CB2) Receptors Activation Protects against Oxidative Stress and Neuroinflammation Associated Dopaminergic Neurodegeneration in Rotenone Model of Parkinson's Disease. *Front. Neurosci.* **2016**, *10*, 321. [CrossRef] [PubMed]
34. Hashiesh, H.M.; Sharma, C.; Goyal, S.N.; Sadek, B.; Jha, N.K.; Kaabi, J.A.; Ojha, S. A focused review on CB2 receptor-selective pharmacological properties and therapeutic potential of β-caryophyllene, a dietary cannabinoid. *Biomed. Pharmacother.* **2021**, *140*, 111639. [CrossRef] [PubMed]
35. Murphy, M.P. Mitochondrial dysfunction indirectly elevates ROS production by the endoplasmic reticulum. *Cell Metab.* **2013**, *18*, 145–146. [CrossRef]
36. Ghosh, A.P.; Klocke, B.J.; Ballestas, M.E.; Roth, K.A. CHOP Potentially Co-Operates with FOXO3a in neuronal cells to regulate PUMA and BIM expression in response to ER stress. *PLoS ONE* **2012**, *7*, e39586. [CrossRef] [PubMed]
37. Klegeris, A.; Bissonnette, C.J.; McGeer, P.L. Reduction of human monocytic cell neurotoxicity and cytokine secretion by ligands of the cannabinoid-type CB2 receptor. *Br. J. Pharmacol.* **2003**, *139*, 775–786. [CrossRef] [PubMed]

38. Vrechi, T.A.M.; Leão, A.H.F.F.; Morais, I.B.M.; Abílio, V.C.; Zuardi, A.W.; Hallak, J.E.C.; Crippa, J.A.; Bincoletto, C.; Ureshino, R.P.; Smaili, S.S.; et al. Cannabidiol induces autophagy via ERK1/2 activation in neural cells. *Sci. Rep.* **2021**, *11*, 5434. [CrossRef]
39. Viscomi, M.T.; Oddi, S.; Latini, L.; Bisicchia, E.; Maccarrone, M.; Molinari, M. The endocannabinoid system: A new entry in remote cell death mechanisms. *Exp. Neurol.* **2010**, *224*, 56–65. [CrossRef]
40. Al Olayan, E.M.; Aloufi, A.S.; AlAmri, O.D.; El-Habit, O.H.; Abdel Moneim, A.E. Protocatechuic acid mitigates cadmium-induced neurotoxicity in rats: Role of oxidative stress, inflammation and apoptosis. *Sci. Total Environ.* **2020**, *723*, 137969. [CrossRef] [PubMed]
41. Namgyal, D.; Ali, S.; Mehta, R.; Sarwat, M. The neuroprotective effect of curcumin against Cd-induced neurotoxicity and hippocampal neurogenesis promotion through CREB-BDNF signaling pathway. *Toxicology* **2020**, *442*, 152542. [CrossRef]
42. Almeer, R.S.; Kassab, R.B.; AlBasher, G.I.; Alarifi, S.; Alkahtani, S.; Ali, D.; Abdel Moneim, A.E. Royal jelly mitigates cadmium-induced neuronal damage in mouse cortex. *Mol. Biol. Rep.* **2019**, *46*, 119–131. [CrossRef] [PubMed]
43. Alnahdi, H.S.; Sharaf, I.A. Possible prophylactic effect of omega-3 fatty acids on cadmium-induced neurotoxicity in rats' brains. *Environ. Sci. Pollut. Res. Int.* **2019**, *26*, 31254–31262. [CrossRef] [PubMed]
44. Elkhadragy, M.F.; Kassab, R.B.; Metwally, D.; Almeer, R.S.; Abdel-Gaber, R.; Al-Olayan, E.M.; Essawy, E.A.; Amin, H.K.; Abdel Moneim, A.E. Protective effects of Fragaria ananassa methanolic extract in a rat model of cadmium chloride-induced neurotoxicity. *Biosci. Rep.* **2018**, *38*, BSR20180861. [CrossRef] [PubMed]
45. Branca, J.J.V.; Morucci, G.; Maresca, M.; Tenci, B.; Cascella, R.; Paternostro, F.; Ghelardini, C.; Gulisano, M.; Di Cesare Mannelli, L.; Pacini, A. Selenium and zinc: Two key players against cadmium-induced neuronal toxicity. *Toxicol. In Vitro* **2018**, *48*, 159–169. [CrossRef] [PubMed]
46. Picciolo, G.; Mannino, F.; Irrera, N.; Altavilla, D.; Minutoli, L.; Vaccaro, M.; Arcoraci, V.; Squadrito, V.; Picciolo, G.; Squadrito, F.; et al. PDRN, a natural bioactive compound, blunts inflammation and positively reprograms healing genes in an "in vitro" model of oral mucositis. *Biomed. Pharmacother.* **2021**, *138*, 111538. [CrossRef]
47. Benvenga, S.; Marini, H.R.; Micali, A.; Freni, J.; Pallio, G.; Irrera, N.; Squadrito, F.; Altavilla, D.; Antonelli, A.; Ferrari, S.M.; et al. Protective Effects of Myo-Inositol and Selenium on Cadmium-Induced Thyroid Toxicity in Mice. *Nutrients* **2020**, *12*, 1222. [CrossRef]
48. Mannino, F.; Imbesi, C.; Bitto, A.; Minutoli, L.; Squadrito, F.; D'Angelo, T.; Booz, C.; Pallio, G.; Irrera, N. Anti-oxidant and anti-inflammatory effects of ellagic and punicic acid in an in vitro model of cardiac fibrosis. *Biomed. Pharmacother.* **2023**, *162*, 114666. [CrossRef]
49. Bitto, A.; Irrera, N.; Pizzino, G.; Pallio, G.; Mannino, F.; Vaccaro, M.; Arcoraci, V.; Aliquò, F.; Minutoli, L.; Colonna, M.R.; et al. Activation of the EPOR-β common receptor complex by cibinetide ameliorates impaired wound healing in mice with genetic diabetes. *Biochim. Biophys. Acta Mol. Basis Dis.* **2018**, *1864*, 632–639. [CrossRef]